

Real-Time Oil Spill Detection with YOLO Framework for Marine Ecosystem Surveillance

Srinivas Talasila^{1*}, Vijaya Kumar Gurralla², Varshini M³, Siva Sai Balla⁴, Madhuri M⁵, and Chinthakindi Kiran Kumar⁶

¹Department of Electronics and Communication Engineering, VNR Vignana Jyothi Institute of Engineering and Technology, Hyderabad, India; Email: srinivas_t@vnrvjiet.in

²Department of Electronics and Communication Engineering, VNR Vignana Jyothi Institute of Engineering and Technology, Hyderabad, India; Email: vijayakumar_g@vnrvjiet.in

³Department of Electronics and Communication Engineering, VNR Vignana Jyothi Institute of Engineering and Technology, Hyderabad, India; Email: varshinics.m@gmail.com

⁴Department of Electronics and Communication Engineering, VNR Vignana Jyothi Institute of Engineering and Technology, Hyderabad, India; Email: madhurigoudmusthyala@gmail.com

⁵Department of Electronics and Communication Engineering, VNR Vignana Jyothi Institute of Engineering and Technology, Hyderabad, India; Email: saishiva216@gmail.com

⁶Department of Electronics and Communication Engineering, Malla Reddy College of Engineering and Technology, Hyderabad, India; Email: ckkmtech11@gmail.com

*Correspondence: Srinivas Talasila; srinivas_t@vnrvjiet.in

ABSTRACT- Early detection of oil spills is crucial and essential for marine environments to minimize environmental harm and enable quick responsive measures. Oil spills can cause significant ecological and financial losses, which emphasizes the need for an efficient monitoring system. This paper presents the use of YOLO deep learning algorithms to enhance the oil spill detection speed and accuracy. A robust and high-quality dataset is taken, consisting of images extracted from Roboflow. To maximize the data quality, preprocessing techniques such as label normalization, contrast enhancement and noise reduction were used. The proposed YOLO algorithms were trained using Adam and SGDM optimizers with an initial learning rate of 0.01, 0.001 and 0.0001. Among the adopted YOLO models, YOLOv9 yielded impressive results with an mAP@0.5 of 94.45%, precision of 95.6%, recall of 93.3% and F1 Score of 94.44%. The recommended system, which incorporates deep learning technologies into marine environment monitoring, greatly improves the marine surveillance systems for oil spill detection and emergency response capabilities by enabling real-time monitoring.

Keywords: Deep Learning, Image Processing, Oil Spill Detection, Marine Ecosystem, YOLO Algorithms.

ARTICLE INFORMATION

Author(s): Srinivas Talasila, Vijaya Kumar Gurralla, Varshini M, Siva Sai Balla, Madhuri M, and Chinthakindi Kiran Kumar;

Received: 20/11/24; **Accepted:** 10/07/25; **Published:** 30/08/25;

E- ISSN: 2347-470X;

Paper Id: IJEER 2011-20;

Citation: 10.37391/ijeer.130310

Webpage-link:

<https://ijeer.forexjournal.co.in/archive/volume-13/ijeer-130310.html>



Publisher's Note: FOREX Publication stays neutral with regard to jurisdictional claims in Published maps and institutional affiliations.

1. INTRODUCTION

Oil spills release petroleum hydrocarbons into the ecosystem, particularly affecting marine environments. Oil spills may lead to environmentally disastrous incidents [1]. In most cases, these oil spills may occur in water, ice, and soil during various stages of oil drilling, extraction, shipping, purification, refining, storing, and supply [2]. These spills lead to substantial impacts on marine environments, and in some cases, disruption of vital processes of ecosystems. Moreover, the effects of oil spillage

not only reach out to the environment, but they can spread their influence beyond those walls into the economic sector and even up to the health sectors of the public. These environmental and socioeconomic problems need immediate action to mitigate the effects and prevent them from having severe repercussions [3]. Oil leak incidents have become more common due to the increasing use of marine transportation. These leaks endanger marine ecosystems as well as human livelihood. Several oil spill exploits were reported in 2023, including a significant spill involving over 700 tons of oil, as well as nine minor exploits ranging from 7 to 700 tons. These nine incidents encompass low-sulfur fuel, gasoline and oil, among other substances. Geographically, there were four incidents recorded in Asia, two in Africa and Europe, and one in America. This trend is very different compared to those recorded in the 2010s [4]. The intensity of such an oil spill into the environment depends on numerous factors, including the chemical composition of the oil, volume spilt, temperature, and wind conditions. An oil slick, which appears as a thin layer on the water's surface after the spill occurs, may expand rapidly and cause environmental damage. To resolve these issues, researchers have investigated advanced technologies, including Artificial Intelligence (AI),

Machine Learning (ML) and Deep Learning (DL), to build systems that are capable of accurately detecting, categorizing, and tracking oil spills on ocean surfaces [5]. The investigation results proved that the developed systems based on computer vision and DL-based approaches greatly improve the performance of the oil spill detection models.

The method applied at present for operational oil spill detection is satellite-based observations supplemented by aerial surveillance. The integration of Synthetic Aperture Radar (SAR) imagery and aerial surveillance can facilitate the achievement of effective monitoring in marine regions. This synergistic approach has proven to be effective in identifying oil spills. Recent studies have clearly shown that polarimetric SAR is capable of distinguishing between oil slicks and biogenic layers. Moreover, polarimetric SAR data can be used to distinguish between genuine oil spills and those that look like oil spills. This poses a huge challenge in oil spill detection [6]. Such advanced technologies increase the precision and reliability of the oil spill monitoring system to a great extent.

2. RELATED WORKS

Oil spillage in marine ecosystems must be monitored and identified efficiently through advanced technologies that offer high precision, flexibility, full automation, and reliable methods. In the past few years, various technologies have been presented, from traditional image processing techniques to advanced machine learning & deep learning technologies. Conventionally, typical image processing methods such as segmentation, edge detection, and thresholding are used for oil spill detection. The utilization of optical and radar satellite imagery has been employed for this purpose. Although these traditional technologies performed well in a controlled environment, they often failed in real-world conditions like sea state, cloud cover, and other environmental changes that degraded the image quality. Since SAR can identify oil spills even in the presence of clouds, it has gained wide usage lately. Still, much scope is left for advanced technologies that may be capable of overcoming the limitations mentioned for detecting thin oil slicks [7]. This section covers a recent overview of the research development made for the identification of oil spills in marine environments.

Tayná et al. [8] aimed to improve the detection and classification accuracy of YOLOv8 algorithm for oil spills in oceans. Authors compared the performance of nano, small and medium versions of YOLOv8. Among them medium version of YOLOv8 achieved better validation results with an accuracy of 0.891, mAP-50 of 0.85 and mAP50-95 of 0.716. A confidence level for detecting objects in the testing phase was more than 70%, indicating the model's efficiency. By addressing the issue of limited availability of real-world oil spill data, Yuepeng Cai et al. [9] developed a novel detection algorithm for small datasets. Landsat-8 satellite oil spill imagery data was utilized to train the model. The original dataset was augmented using a single image generative adversarial network (SiGAN). SiGAN will generate multi-shaped oil spill samples from a single image by gaining texture information from multiple scales. The YOLOv8 model was trained using transfer learning on both

original and augmented datasets. The experimental results showed that the augmented dataset improves recall by 12.3%, precision by 6.3% and average precision by 11.3%.

Shanmukh et al. [10] evaluated the three semantic segmentation algorithms: PSPNet, DeepLabV3 and FCN with U-Net for segmenting oil spill regions. SAR images were used for the work. Performance metrics such as pixel-wise accuracy and Intersection over Union (IoU) were calculated to assess the model's performance. U-Net achieved better IoU with a segmentation accuracy of 95%, yet FCN and U-Net performed well in identifying oil spills. Overcoming the limitations of conventional imaging techniques, such as visual, hyperspectral and microwave, sensing techniques like polarimetric and thermal imaging offer improved detection accuracy.

The purpose of the research conducted by Trongtirakul et al. [11] is to examine the potential of using thermal and polarimetric imaging to monitor oil spills in 3-D dimensions. This proposed system suggests an unsupervised learning algorithm to improve detection capability. The proposed framework consists of a segmentation network for spills specifically designed for thermal and polarimetric imaging, 3D visualization of oil thickness and a multi-density oil spill region extraction algorithm, and an approach that analyses oil spills quantitatively and qualitatively. The developed system has been validated through comparisons with the current approaches, leading to the development of more effective and reliable systems for detecting and monitoring oil spills. Improving the SAR image processing methods for environmental monitoring and protecting the marine ecosystem, Patel et al. [12] developed a deep learning algorithm using EMAS dataset. The designed system uses a 23-layer CNN network to classify oil spill patches into less than 0.5% and more than 0.5% oil spill pixels, followed by a U-Net network to segment those patches. Hasimoto-Beltran et al. [13] presented a novel oil spill segmentation network named Multichannel Deep Neural Network (M-DNN). This network was trained and tested on SAR imagery. The proposed M-DNN outperforms the Single Channel DNN with pixel accuracy of 98.56% and 14-times faster convergence than earlier approaches. Sun et al. [14] examine the effectiveness of three CNN architectures: U-Net, BiSeNetV2, and DeepLabV3+ for identification of oil spills using medium-resolution optical satellite images. These images are captured from Sentinel-2 MSI, Landsat-8 OLI, and Landsat-9 OLI2. The adopted CNNs' performance was increased using SE, CBAM and SimAM modules. The U-Net with CABM module achieved greater performance than the others.

In this study, we introduced YOLOv9 deep learning model for an oil spill detection system. The YOLOv9 model was chosen since it analyzes the data quickly and more accurately than earlier YOLO versions for the task. The model was trained on high-resolution ocean images consisting of oil spills. RGB images were utilized for the work to extract features for detection, unlike SAR-based detection methods that utilize backscatter coefficients. Preprocessing techniques such as contrast enhancement, noise reduction and optimization were applied for increased accessibility of the data to maximize the

detection performance. The proposed model can effectively identify oil spills even under various environmental conditions.

3. PROPOSED METHODOLOGY

The main aim of this research is to create a deep-learning model for identifying oil spills in marine environments. This was accomplished by exploring advanced object-detection frameworks, which also apply a deep learning model that excels in recognizing patterns and making predictions from complex, high-dimensional data such as images, audio, and text. The YOLO (You Only Look Once) object detection algorithm is

capable of detecting many objects in one single image and also maintains real-time efficiency with high precision; hence, it is highly preferred for detection purposes. Due to its competency in detecting many objects within a single image, this algorithm is most suitable for environmental monitoring and conservation-based tasks. Thus, the selected dataset was used for training several versions of YOLO, enabling highly accurate and precise detection of oil spills, making them ideal models for environmental safety concerns.

The workflow for training the adopted object detection models for oil spills in marine environments is shown in *figure 1*.

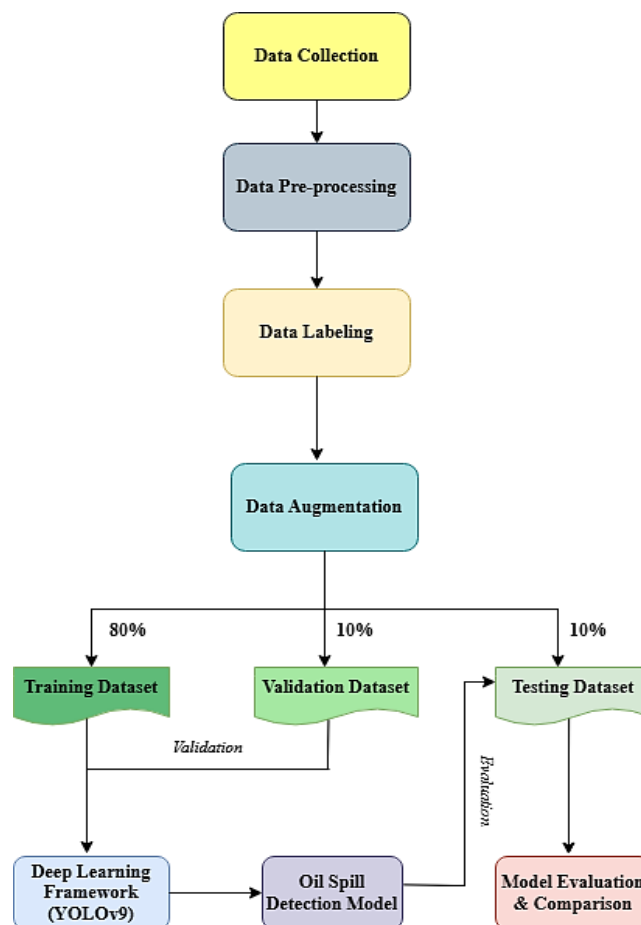


Figure 1. Workflow of the proposed oil spill detection system

3.1. Data Collection

The images in the dataset were sourced from Roboflow and grouped into two categories such as oil and no oil. This dataset contains a total of 1564 images, which were further divided into training, validation and testing sets [15]. The resolution of the images in the dataset are resized to 640×640 for further analysis. An 80:10:10 split ratio was utilized to train the model. So, 1252 images allotted for training, 156 for validation and 156 for testing. All the images in the dataset were annotated manually to mark the affected oil spill areas by drawing bounding boxes around the polluted regions. This process enables the trained

model to distinguish the oil spill regions and normal ocean surfaces more effectively.

The sample original images and annotated images are shown in *figure 2*. After annotation, a few augmentation techniques are applied, including adjusting the saturation ranging from -25% to 25% to replicate variable color intensities and exposure shift ranging from -10% to +10% to approximate various lighting conditions. A Gaussian blur of up to 1px is also used to imitate camera defocus or motion blur. Two augmented output samples are created from each training sample to enhance the dataset and prevent overfitting.

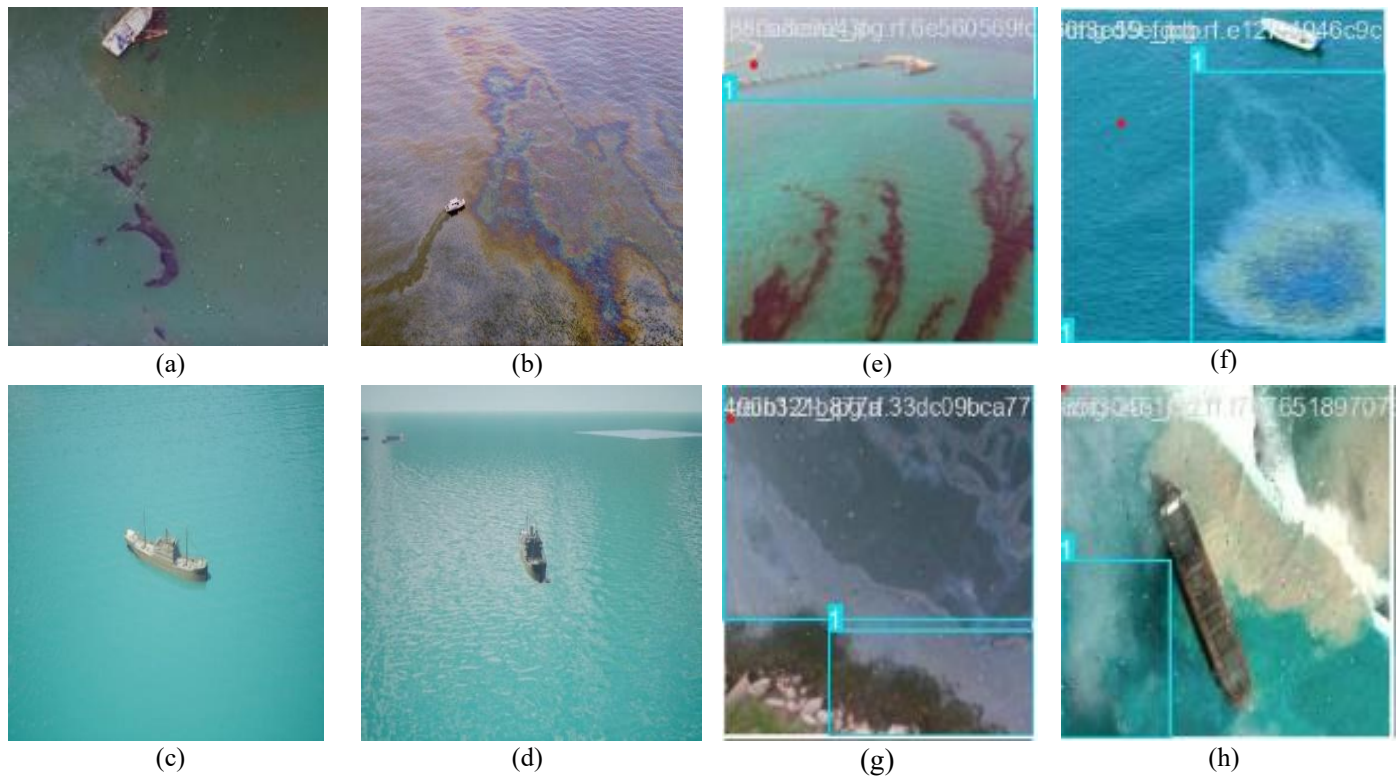


Figure 2. Sample images in the dataset: (a-b) – Oil Spills, (c-d) – No Spill, (e-f) annotated samples

#Algorithm: Real-time Oil Spill detection using YOLOv9 model

Begin

Dataset Collection: $dataset \leftarrow \text{Collect oil spill images and annotations}$

Preprocessing: $preprocessed_data \leftarrow \text{PreprocessData}(dataset)$

Labeling: $labeled_data \leftarrow \text{LabelImages}(preprocessed_data)$

Augmentation:
 $augmented_data \leftarrow \text{AugmentData}(labeled_data)$

Data Splitting: $training_data, validation_data, testing_data \leftarrow \text{SplitData}(augmented_data, 80\%, 10\%, 10\%)$

Model Selection and Training:
 $model \leftarrow \text{InitializeYOLOv9}()$

$trained_model \leftarrow \text{TrainModel}(model, training_data, validation_data)$

Model Evaluation: $Performance\ Metrics \leftarrow \text{EvaluateModel}(oil_spill_model, testing_data)$

Comparison with other models:
 $\text{CompareWithOtherModels}(YOLOv9, YOLOv8, YOLOv5)$

End

3.2. YOLO

YOLO operates as a unified approach, processing an entire image in a single forward pass through the network [16]. This “one-step” approach enables YOLO to detect multiple objects in a single image with exceptional speed and accuracy. YOLO models are pre-trained on huge datasets such as COCO, which is particularly collected with the intention of including a wide range of objects for real-world identification and classification. With more than 80 divergent categories of objects, the COCO dataset provides a robust foundation for the deployment of YOLO architecture in complex and diverse scenarios. Pre-training on large datasets like COCO helps YOLO perform generalization better across a number of tasks, thus increasing its applicability for customizable object detection by finetuning on specific datasets. The YOLO model typically segments the image into a grid comprising $S \times S$ cells. Each cell predicts a constant number of bounding boxes with their scores. The scores denote the probability that a bounding box contains an object. Moreover, YOLO predicts class probabilities for every detected bounding box so that it can predict the object accurately.

The key formula used in YOLO to calculate the confidence score for each bounding box is:

$$C_i = P(object) \times IoU_{pred, truth} \quad (1)$$

Where, $P(object)$ represents the probability that an object exists within the bounding box and $IoU_{pred, truth}$ represents Intersection over Union (IoU) between the predicted bounding box and the ground truth bounding box.

During training, YOLO minimizes the Mean Square Error (MSE) between the predicted bounding box coordinates, confidence scores, class probabilities, and ground truth values. The total loss function, denoted as L , combines errors from three key sources. First, the localization loss captures the error in the bounding box coordinates. Second, the confidence loss reflects the error in estimating the probability that an object exists within the bounding box. Finally, the classification loss accounts for the error in predicting the correct class of the detected object. The total loss is defined as:

$$L = \lambda_{coord} \sum_{i=0}^{S^2} \sum_{j=0}^B 1_{ij}^{obj} [(x - \hat{x})^2 + (y - \hat{y})^2 + (w - \hat{w})^2 + (h - \hat{h})^2] + \sum_{i=0}^{S^2} \sum_{j=0}^B 1_{ij}^{obj} [(C - \hat{C})^2] \quad (2)$$

Where, λ_{coord} is a parameter that emphasizes the localization loss. The variables x, y, w , and h represents the bounding box, where x, y are the center of the box and w, h are width and height of the box. $\hat{x}, \hat{y}, \hat{w}, \hat{h}$ are predicted bounding box coordinates. C is the confidence score and \hat{C} is the predicted confidence score. The indicator function 1_{ij}^{obj} is equal to 1 if an object appears in cell i with box j , and 0 if it does not.

3.3. YOLOv9

YOLOv9 [17] was chosen for this work due to its superior performance in terms of accuracy and speed among the previous versions like YOLOv5, YOLOv8, etc., and other object detection models like SSD and Faster R-CNN. The deciding factor for YOLOv9 for this work is its capability to detect small objects when dealing with the scattering areas in large satellite images, particularly for oil spills in marine environments. YOLOv9 introduces Generalized Efficient Layer Aggregation Network (GELAN) as the backbone to improve gradient propagation and feature aggregation by sustaining the computation efficiency, compared to its earlier versions. The optimized structure for its backbone improves and strengthens the feature extraction ability, making differences between different types of oil spills. To make the training process more stable and enhance the model's generalizability, YOLOv9 incorporated a Programmable Gradient Information (PGI) strategy and drop-path regularization. Unlike YOLOv8, YOLOv9 uses task-aligned assignment strategies for detection to boost the precision for small and complex objects. Moreover, the improved loss functions covering localization, classification, and confidence significantly increased the accuracy of bounding box predictions, thus reducing both false positives and false negatives, ensuring reliable detection in challenging environments.

4. RESULTS AND DISCUSSION

Three YOLO versions: YOLOv5, YOLOv8 and YOLOv9 were used and finetuned for the task of detecting oil spills in marine environments. All the models were trained using different initial learning rates and optimizers to obtain the best model for detection. The trained models were assessed using performance *Metrics*: mean average precision, precision, recall and F1 score.

A comprehensive comparison between the adopted YOLO model's performance is provided in this section.

4.1. Hyperparameter Setting

The adopted model was fine-tuned using pre-trained weights and trained on a custom dataset for oil spill detection. The key hyperparameters set during the model training are optimizer, batch size, learning rate, and number of epochs. For this work, the batch size, which defines the number of images processed at a time during the training, was set to 16. The learning rate, which determines the speed of weight updates during optimization, was set to the values 0.01, 0.001 and 0.001. Optimizers such as SGDM and Adam were employed and trained the models for 60 epochs. GPU accelerated environment in Google Colab was used for the training process to facilitate quick training.

4.2. Performance Metrics

To compute the performance metrics, four key computations are required. Those are TP, TN, FP, and FN. TP is the number of true positives (correctly predicted oil spills), TN is the number of true negatives (correctly predicted non-oil regions), FP is the number of false positives (non-oil regions incorrectly predicted as oil spills), FN is the number of false negatives (oil spills incorrectly predicted as non-oil regions).

mAP@0.5: It is a measure that gives the accuracy of the model in locating and correctly identifying oil spills in images. Also defined as the mean of area under the precision and recall curve for all classes at IoU threshold 0.5.

Precision: The ratio of true positives, *i.e.*, oil spills correctly identified as oil spills by the model to the sum of true positives and false positives, *i.e.*, the total number of instances identified as oil spills.

$$Precision = \frac{TP}{TP + FP}$$

Recall: The ratio of true positives, *i.e.*, oil spills correctly identified as oil spills by the model to the sum of true positives and false negatives, *i.e.*, oil spills correctly identified as oil spills and oil spills incorrectly identified as non-oil spills by the model.

$$Recall = \frac{TP}{TP + FN}$$

F1 Score: The harmonic mean of precision and recall, which provides a balance between these two metrics.

$$F1\ Score = \frac{2 * Precision * Recall}{Precision + Recall}$$

4.3. Experimental Results

The performance of YOLOv5 for oil spill detection was assessed using two optimizers and three initial learning rates, achieving the best performance when model was trained on Adam optimizer at a learning rate of 0.001. Under these conditions, YOLOv5 achieved an mAP@0.5 of 92.7%, precision of 96.6%, recall of 88.8% and F1 score of 92.63%.

Conversely, results obtained by using the SGDM optimizer were significantly lower than Adam optimizer across all the initial learning rates. The evaluation results of YOLOv5 across various hyperparameter combinations are represented in *fig. 3*.

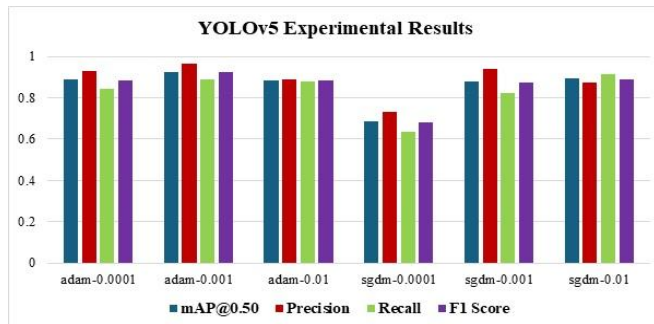


Figure 3. Comparison of YOLOv5 Performance at Various Hyperparameter Combinations

For YOLOv8, the evaluation results showed that Adam optimizer attained optimal performance when initial learning rate was set to 0.001. This combination achieved mAP@0.5 of 94.28%, precision of 95.1%, recall of 93.3% and F1 score of 94.18%. On the other hand, SGDM achieved slightly lower performance compared to Adam when initial learning rate was set to 0.01, and achieved an mAP@0.5 of 93.25%. The evaluation results of YOLOv8 across various hyperparameter combinations are represented in *fig. 4*.

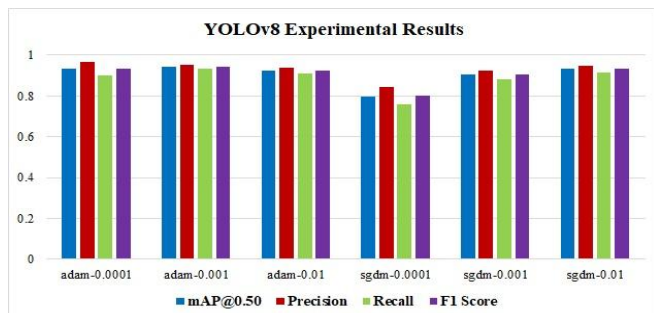


Figure 4. Comparison of YOLOv8 Performance at Various Hyperparameter Combinations

YOLOv9 exhibited better and almost equal performance using both Adam and SGDM when fine-tuning at initial learning rate of 0.001. The Adam optimizer achieved an mAP@0.5 of 94.45%, precision of 95.6%, recall of 93.3% and F1 score of 94.44%, whereas sgdm optimizer achieved the same accuracy, precision and recall but F1 score of 94.31%, demonstrating its robust performance and highlighting its capability as an alternative option. The evaluation results of YOLOv9 across various hyperparameter combinations are represented in *fig. 5*.

The normalized confusion matrix shown in *fig. 6* highlights the performance of YOLOv9 model for oil spill detection. The model accurately identified 91% of no-oil spills and 97% of oil spills, exhibiting minimal misclassification of 3% false positives and 3% false negatives. Higher accuracy in detecting and a minimal error rate indicate the proposed model is a

reliable choice for real-time environmental monitoring, providing efficient detection of oil spills in oceans.

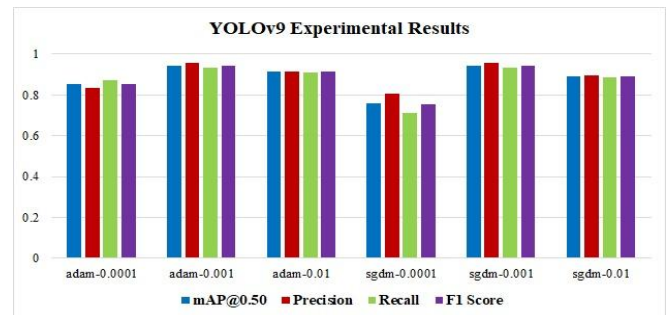


Figure 5. Comparison of YOLOv8 Performance at Various Hyperparameter Combinations

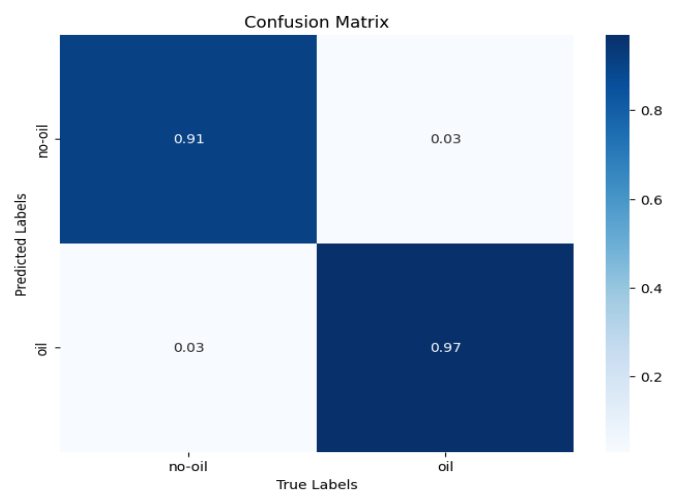


Figure 6. Confusion matrix of YOLOv9 on the test set

Moreover, using YOLOv9 achieved an average performance of 88.44%, which shows the consistency of the model's performance across multiple runs. And also, to understand the variability, computed the standard deviation, which was 0.0677, indicating very slight variations in performance between the runs. The confidence interval obtained, ranging from 0.8134 to 0.9554, indicates that the model's average performance lies within this range across multiple runs.

The strengths and limitations of oil spill detection using YOLO algorithms, particularly using YOLOv5, YOLOv8 and YOLOv9 were comprehended by assessing their performance at various hyperparameter combinations. YOLOv5 version with Adam outperformed against SGDM. YOLOv8 showed a significant increase in performance over YOLOv5 in all the combinations. The findings of YOLOv8 highlight its ability to handle more complex tasks. YOLOv9 is the most advanced version, achieved a greater performance and demonstrated its superiority in accuracy, precision, recall and F1 score. YOLOv9's enhanced feature extraction capability and optimized loss function enable it to be adopted for detecting oil spills more effectively in large and complex satellite images. The comparison of the performance of three adopted YOLO models is presented in *table 1*.

Table 1. Performance comparison of the trained models

Model	mAP@0.5	Precision	Recall	F1 Score
YOLOv5	0.927	0.966	0.888	0.9263
YOLOv8	0.9428	0.951	0.933	0.9418
YOLOv9	0.9445	0.956	0.933	0.9444

By keeping the challenges in mind that can make it difficult to spot actual oil spills, such as waves, sunlight reflections, and sea clutter, the proposed model uses a real-time dataset. As the dataset has a wide variety of ocean images, the suggested YOLOv9 model effectively recognizes the difference between normal sea patterns and oil spills. In many cases, spills may be partially hidden by boats, ships, oil rigs, etc. The presented object detection algorithm is well-suited to localizing the oil spills even when only the parts of the oil spills are visible.

Oceans look totally different in bright sunlight and under clouds. Our model has been trained to recognize spills using data augmentation techniques like brightness and saturation changes, making it more adaptable to different lighting changes. Finally, our developed YOLOv9 model is robust and reliable for oil spill detection in real-time marine environments.

Even though the results obtained in this work are optimal, there are still some limitations that can be optimized in the future. The data set utilized in this work has a limited number of images, *i.e.*, 1564 images, which may affect real-time performance. Additionally, most of the images in the dataset are collected from publicly available sources where real-world variability is absent. Including satellite or Synthetic Aperture Radar images in the current dataset in the future may enhance the generalization of the model. This facilitates the model to detect oil spills under various challenging conditions.

5. CONCLUSION

This study explored the use of YOLO deep learning models for the detection of oil spills in aquatic environments. Efficient oil spill detection necessitates quick and accurate systems to ensure timely environmental monitoring and catastrophe control. Experimental findings indicate that YOLOv9 model with optimized hyperparameters significantly improves the detection performance. Utilizing a comprehensive dataset of oil spill images, the model accurately identifies oil spills, surpassing the traditional approaches. The mean average precision of YOLOv9, which is 94.45%, indicates that it is a reliable and efficient choice for real-time oil spill monitoring. As future work, we will focus on increasing the dataset size to include images under varied environmental conditions and optimizing the algorithms to enhance usability for the users. Furthermore, using alternative deep learning technologies may enhance this methodology, enabling the further use of automation methods in environmental research to safeguard natural resources.

Conflicts of Interest: The authors declare no conflict of interest.

REFERENCES

- [1]. Akhmedov, F., Nasimov, R., & Abdusalomov, A. (2024). Developing a comprehensive oil spill detection model for marine environments. *Remote Sensing*, 16(16), 3080. <https://doi.org/10.3390/rs16163080>.
- [2]. Khalturin, A. A., Parfenchik, K. D., & Shpenst, V. A. (2023b). Features of oil spills monitoring on the water surface by the Russian Federation in the Arctic Region. *Journal of Marine Science and Engineering*, 11(1), 111. <https://doi.org/10.3390/jmse11010111>.
- [3]. Vasconcelos, R. N., Lima, A. T. C., Lentini, C. a. D., Miranda, J. G. V., De Mendonça, L. F. F., Lopes, J. M., Santana, M. M. M., Cambuí, E. C. B., Souza, D. T. M., Costa, D. P., Duverger, S. G., & Franca-Rocha, W. S. (2023). Deep Learning-Based Approaches for Oil Spill Detection: A Bibliometric review of research trends and challenges. *Journal of Marine Science and Engineering*, 11(7), 1406. <https://doi.org/10.3390/jmse11071406>.
- [4]. ITOPF. (n.d.). Oil tanker spill Statistics 2023 - ITOPF. <https://www.itopf.org/knowledge-resources/data-statistics/statistics>.
- [5]. V, S., & Saro, V. A. (2024). OSD-DNN: Oil Spill Detection using Deep Neural Networks. *International Journal of Performativity Engineering*, 20(2), 57. <https://doi.org/10.23940/ijpe.24.02.p1.5767>.
- [6]. Gui, S., Song, S., Qin, R., & Tang, Y. (2024). Remote Sensing Object Detection in the Deep Learning Era—A Review. *Remote Sensing*, 16(2), 327. <https://doi.org/10.3390/rs16020327>.
- [7]. Amani, M., Mehravar, S., Asiyabi, R. M., Moghimi, A., Ghorbanian, A., Ahmadi, S. A., Ebrahimi, H., Moghaddam, S. H. A., Naboureh, A., Ranjgar, B., Mohseni, F., Nazari, M. E., Mahdavi, S., Mirmazloumi, S. M., Ojaghi, S., & Jin, S. (2022). Ocean Remote Sensing Techniques and Applications: A Review (Part II). *Water*, 14(21), 3401. <https://doi.org/10.3390/w14213401>.
- [8]. Tayná Cristina Sousa Silva, Monik Silva Sousa, & João Viana da Fonseca Neto. (2024). Deep Learning for Oil Spill Detection and Classification in Ocean Surface. *International Journal of Advances in Engineering and Technology*, 17(1), 13–24. <https://doi.org/10.5281/zenodo.10860934>.
- [9]. Cai, Y., Chen, L., Zhuang, X., & Zhang, B. (2024). Automated marine oil spill detection algorithm based on single-image generative adversarial network and YOLO-v8 under small samples. *Marine Pollution Bulletin*, 203, 116475. <https://doi.org/10.1016/j.marpolbul.2024.116475>.
- [10]. M. P. Shanmukh, S. B. Priya and T. Madeswaran, "Improving Oil Spill Detection in Marine Environments Through Deep Learning Approaches," 2024 Fourth International Conference on Advances in Electrical, Computing, Communication and Sustainable Technologies (ICAECT), Bhilai, India, 2024, pp. 1-6, doi: 10.1109/ICAECT60202.2024.10468888.
- [11]. T. Trongtirakul, S. Agaian, A. Oulefki and K. Panetta, "Method for Remote Sensing Oil Spill Applications Over Thermal and Polarimetric Imagery," in *IEEE Journal of Oceanic Engineering*, vol. 48, no. 3, pp. 973-987, July 2023, doi: 10.1109/JOE.2023.3245759.
- [12]. Patel, K., Bhatt, C., Corchado, J.M. (2023). Automatic Detection of Oil Spills from SAR Images Using Deep Learning. In: Julián, V., Carneiro, J., Alonso, R.S., Chamoso, P., Novais, P. (eds) *Ambient Intelligence—Software and Applications—13th International Symposium on Ambient Intelligence. ISAmI 2022. Lecture Notes in Networks and Systems*, vol 603. Springer, Cham. https://doi.org/10.1007/978-3-031-22356-3_6.
- [13]. Hasimoto-Beltran, R., Canul-Ku, M., Méndez, G. M. D., Ocampo-Torres, F. J., & Esquivel-Trava, B. (2023). Ocean oil spill detection from SAR images based on multi-channel deep learning semantic segmentation. *Marine Pollution Bulletin*, 188, 114651.
- [14]. Sun, Z., Yang, Q., Yan, N., Chen, S., Zhu, J., Zhao, J., & Sun, S. (2024). Utilizing deep learning algorithms for automated oil spill detection in

medium resolution optical imagery. Marine Pollution Bulletin, 206, 116777.

- [15]. Retrieved from Roboflow: <https://universe.roboflow.com/yolo-m1lmy/oil-detection-2>
- [16]. J. Redmon, S. Divvala, R. Girshick and A. Farhadi, "You Only Look Once: Unified, Real-Time Object Detection," 2016 IEEE Conference on Computer Vision and Pattern Recognition (CVPR), Las Vegas, NV, USA, 2016, pp. 779-788, doi: 10.1109/CVPR.2016.91.
- [17]. Wang, CY., Yeh, IH., Mark Liao, HY. (2025). YOLOv9: Learning What You Want to Learn Using Programmable Gradient Information. In: Leonardis, A., Ricci, E., Roth, S., Russakovsky, O., Sattler, T., Varol, G. (eds) Computer Vision – ECCV 2024. ECCV 2024. Lecture Notes in Computer Science, vol 15089. Springer, Cham. https://doi.org/10.1007/978-3-031-72751-1_1.



© 2025 by Srinivas Talasila, Vijaya Kumar Gurrula, Varshini M, Siva Sai Balla, Madhuri M, and Chinthakindi Kiran Kumar. Submitted for possible open access publication under the terms and conditions of the Creative Commons Attribution (CC BY) license (<http://creativecommons.org/licenses/by/4.0/>).